

**Lawrence Berkeley National Laboratory**  
Lawrence Berkeley National Laboratory

**Title**

KINETICS OF IRON - SODIUM DISILICATE REACTIONS AND WETTING

**Permalink**

<https://escholarship.org/uc/item/8t59660r>

**Author**

Tomsia, Antoni P.

**Publication Date**

1980



# Lawrence Berkeley Laboratory

UNIVERSITY OF CALIFORNIA

## Materials & Molecular Research Division

Submitted to the Journal of the American Ceramic  
Society

KINETICS OF IRON - SODIUM DISILICATE REACTIONS  
AND WETTING

Antoni P. Tomsia and Joseph A. Pask

January 1980

RECEIVED  
LAWRENCE  
BERKELEY LABORATORY

APR 7 1981

LIBRARY AND  
DOCUMENTS SECTION

**For Reference**

Not to be taken from this room



LBL-10443 c.1

## DISCLAIMER

This document was prepared as an account of work sponsored by the United States Government. While this document is believed to contain correct information, neither the United States Government nor any agency thereof, nor the Regents of the University of California, nor any of their employees, makes any warranty, express or implied, or assumes any legal responsibility for the accuracy, completeness, or usefulness of any information, apparatus, product, or process disclosed, or represents that its use would not infringe privately owned rights. Reference herein to any specific commercial product, process, or service by its trade name, trademark, manufacturer, or otherwise, does not necessarily constitute or imply its endorsement, recommendation, or favoring by the United States Government or any agency thereof, or the Regents of the University of California. The views and opinions of authors expressed herein do not necessarily state or reflect those of the United States Government or any agency thereof or the Regents of the University of California.

# KINETICS OF IRON - SODIUM DISILICATE REACTIONS AND WETTING

Antoni P. Tomsia and Joseph A. Pask

Materials and Molecular Research Division, Lawrence Berkeley Laboratory  
and Department of Materials Science and Mineral  
Engineering, University of California  
Berkeley, CA 94720

## ABSTRACT

Thermogravimetric and sessile drop measurements were used to study kinetics of redox reactions between sodium disilicate glass and iron. Two redox reaction sequences were identified; both introduced ferrous oxide into the glass at the interface. One consists of formation of ferrous oxide at the interface by reduction of sodium ions in the glass; this is primarily dependent on the  $a(\text{FeO})$  in the metal being less than one. The second consists of oxidation of ferrous ions in the glass by the reduction of sodium ions to form ferric ions which subsequently react with the iron to form ferrous oxide. The reaction rates were shown to be sensitive to temperature, time, total ambient pressure, partial pressure of sodium and oxygen in the atmosphere and the  $a(\text{FeO})$  in the iron. Decrease of contact angles and spreading occurs with the redox reaction in which the metal plays an active role, i.e. whose  $a(\text{FeO})$  is less than one and whose composition undergoes a change.

This work was supported by the Director, Office of Energy Research, Office of Basic Energy Sciences, Materials Science Division of the U.S. Department of Energy under Contract No. W-7405-ENG-48.

## I. INTRODUCTION

The theory of glass to metal bonding developed in this laboratory states that chemical bonding, or maximum adherence, occurs at the interface when chemical equilibrium is realized by saturation of the interfacial zone with the lowest valence oxide of the metallic phase. The thermodynamic activity of the lowest valence metal oxide in this zone is thus one. This condition results in a balance of bond energies and a continuous electronic structure across the interface, i.e., a chemical bond. These concepts have been developed from wetting and reaction studies of sodium silicates on Fe, Ni, Co, Au and Pt, and on Ni<sub>50</sub>Fe<sub>50</sub> and Ni<sub>50</sub>Co<sub>50</sub> alloys<sup>(1-3)</sup>.

Since chemical thermodynamic equilibrium seldom exists initially between most metal and glass systems, reactions occur after intimate interfaces are formed. It is important to understand these reactions and the conditions under which they occur, because they lead to saturation of the interfacial zone with the oxide of the substrate metal. This study was undertaken to evaluate the nature of the reactions between iron and sodium disilicate (NS<sub>2</sub>) as a function of time, temperature, and nature of the ambient atmosphere.

## II. EXPERIMENTAL

### A. Materials

Marz A iron in 0.254 mm thick foils was obtained from Materials Research Corporation, Orangeburg, N.Y., and was 99.995% pure as specified. The major reported impurities were carbon (8 ppm) and oxygen (~60 ppm). Armco iron was obtained in the form of sheet of 1 mm thickness of reported

99.8% purity with a typical analysis of 0.015% C, 0.025% MN, 0.005% P, 0.025% S, 0.002% Si. Precipitates of FeO were detected metallographically. All metal samples were cut into 12 x 12 mm squares. The metal plates were then polished through a set of dry polishing papers and given a final high metallurgical polish on a lap wheel with 0.3  $\mu$ m alumina. All samples were cleaned in distilled water, ethyl alcohol and acetone in ultrasonic cleaner. Samples were prepared immediately prior to an experiment.

A sodium disilicate glass (NS<sub>2</sub>-LBL) was prepared in our laboratory from reagent grade sodium carbonate and fused silica glass #7940 (Corning Glass Works, -325 mesh). Batch materials to yield 250 grams of glass were mixed with isopropyl alcohol for 24 hrs, slowly dried at 60°C, melted at 1350°C in air for 3 hrs with occasional stirring in a platinum crucible, cooled and crushed. The glass was remelted twice to ensure homogeneity. The final melt was held at 1200°C for 12 hrs to remove bubbles and then poured into a heated graphite mold. After annealing the glass at 500°C for 2 hrs, it was cut under kerosene with a diamond saw to cubes with a nominal edge size of  $2.0 \pm 0.1$  mm and a weight of  $200 \pm 2$  mg, and stored in a laboratory vacuum desiccator until used. The chemical analysis of NS<sub>2</sub>-LBL as well as other glasses used in this study is presented in Table I.

#### B. Experimental Apparatus

Two vacuum furnaces were used in order to perform experiments at two partial pressures of oxygen,  $P_{O_2}$ . The first, which shall be referred to as graphite furnace, had an estimated  $P_{O_2}$  of  $\approx 10^{-17}$  Pa which was

below the dissociation pressure of ferrous oxide. At 1000°C the dissociation pressure for bulk FeO is  $1.5 \times 10^{-10}$  Pa and for bulk  $\text{Fe}_2\text{O}_3$ ,  $6.4 \times 10^{-10}$  Pa. It consisted of a graphite tube resistance heating element inside of which was an alumina D-tube on which the specimen was placed. It has been previously described<sup>(4)</sup>. The experimental vacuum chamber was connected to an inert gas supply and an oil diffusion pump capable of a vacuum of up to  $\approx 10^{-5}$  Pa. Contact angle measurements within  $\pm 1^\circ$  were made by sighting along the alumina D-tube through fused silica windows in the vacuum chamber with a telescope equipped with a goniometer.

The second furnace, which shall be referred to as alumina furnace, had an estimated  $P_{\text{O}_2}$  of  $\approx 10^{-7}$  Pa which was above the dissociation pressure of ferrous oxide. It consisted of a one inch diameter, eight inch long Kanthal wire-wound high density alumina tube (Fig. 1). The furnace was inside a large vacuum chamber that had a vacuum capability of  $\approx 10^{-5}$  Pa. Both ends of the furnace tube were kept open. A leak valve on the vacuum chamber allowed inert gases to be introduced into the furnace. The contact angles were measured through a porthole in the vacuum chamber with a telegoniometer. A camera was attached to the telegoniometer through which pictures of the substrates and drops were taken.

The ambient pressures in both furnaces were measured with a calibrated cold-cathode ionization gage. A liquid nitrogen cold trap was used to condense vapors from the diffusion pump. Most of the experiments were carried out at  $2.6 \times 10^{-4}$  Pa at the test temperature.

The temperature in both furnaces was measured with two Pt-Pt 10% Rh thermocouples which were calibrated at four temperatures against the melting points of single crystals of KCl, NaCl, LiF and  $\text{MgF}_2$ . The

accuracy of temperature control was  $\pm 2^\circ\text{C}$ .

### C. Experimental Procedure

The glass cube and metal plate assemblies were weighed before and after each sessile drop experiment. The loss in weight was calculated as the percent of the total Na in the glass lost by redox reactions to be described later. The procedure for a test consisted of first pumping the system down to  $<2.6 \times 10^3 \text{Pa}$ , then pumping with a cold-trapped diffusion pump to  $<1.3 \times 10^{-4} \text{Pa}$ , heating to the test temperature (e.g., with a schedule of 30 min. to  $600^\circ\text{C}$  and 10 more min. to  $1000^\circ\text{C}$ ), holding for the test time and furnace cooling ( $500^\circ\text{C}$  in 5 - 15 min.).

The surface of the substrates, particularly at the periphery of the drop, was examined by metallographic and scanning electron microscopy. Selected specimens were cut with a diamond saw on a plane perpendicular to the metal-glass interface. After mounting in bakelite, cross-sections were polished on dry emery papers and on a lap wheel with  $0.3 \mu\text{m}$  alumina and finally with  $0.05 \mu\text{m}$  alumina. All specimens were then etched in 10% HF solution for 10 seconds.



Cross-sections were examined with a metallographic and a scanning electron microscope with EDAX capability. Qualitative information on adherence, which was adequate for this study, was obtained by subjecting some of the specimens to bending: poor adherence was associated with the glass cleanly separating from the metal substrate and good adherence, with the glass fracturing.

### III. RESULTS

#### A. Experiments with Marz A Iron

Sessile drop experiments at an ambient pressure of  $2.6 \times 10^{-4}$  Pa of NS<sub>2</sub>-LBL glass on Marz A iron were made at 900 to 1000°C at increments of 20°, each for 120 min (Fig. 2). A second series was made at 1000°C for times of 30 to 240 min at increments of 30 min (Fig. 3). The figures show the contact angles obtained in both the alumina ( $P_{O_2} \cong 10^{-7}$  Pa) and graphite ( $P_{O_2} \cong 10^{-17}$  Pa) furnaces. The contact angle decreased with temperature and time, with spreading (indicated by a reported zero contact angle) occurring only in the graphite furnace at 1000°C after 90 or more minutes.

Figures 2 and 3 also show corresponding weight loss data for each point expressed as percent of total Na in the starting glass. Loss of Na was verified by chemical analysis of deposits that formed on the colder parts of the furnace including the viewing ports; the deposits were initially metallic in appearance and oxidized on exposure to air. Weighings before and after a test were always made of the glass drop with its substrate. The weight loss in the graphite furnace under similar temperature, time and total ambient pressure conditions was always greater than in the alumina furnace. A weight loss also indicated reactions since a blank

substrate of Marz A iron and NS<sub>2</sub>-LBL glass on Pt or fused SiO<sub>2</sub> substrate in either furnace at 1000°C for 1 or 2 hrs showed no weight changes (Table 2).

This data indicated the occurrence of continuing redox reactions at the interface involving replacements of 2Na<sup>+</sup> in the glass by Fe<sup>+2</sup> by the transfer of 2 electrons from an Fe atom to 2Na<sup>+</sup> which become 2Na atoms. Further verification of the occurrence of reactions was the development of a bluish color by the glass and the appearance of cristobalite (SiO<sub>2</sub>) precipitates after about 65 wt% of the overall starting Na was lost, and also of fayalite (2FeO·SiO<sub>2</sub>) after about 79 wt% loss. These crystalline phases were identified by x-ray diffraction analyses of powdered specimens.

Examination of the 1000°C isothermal section of the Na<sub>2</sub>O-FeO-SiO<sub>2</sub> phase equilibrium diagram (Fig. 4) supports this phase sequence<sup>(2,8)</sup>. Replacement of 2xNa<sup>+</sup> in the NS<sub>2</sub> liquid with xFe<sup>+2</sup> results in a change of composition with the liquid becoming saturated with SiO<sub>2</sub> after 70.5% loss of the total Na. Continued replacement of Na<sup>+</sup> causes continued precipitation of SiO<sub>2</sub> and change of the liquid composition to 5.4 wt% Na<sub>2</sub>O and 31.1 wt% FeO when the liquid also becomes saturated with FeO, and further replacement of 2Na<sup>+</sup> by Fe<sup>+2</sup> causes continued precipitation of cristobalite and fayalite with a decrease of the amount of liquid but with no change in its composition. The smaller amounts of Na lost experimentally before the appearance of the precipitate were due to kinetic and geometric factors generated by the fact that the actual reaction was occurring at a single interface with diffusion, and possibly because of the appearance of some Fe<sup>+3</sup> in the glass composition to be discussed later.

Further evidence for the occurrence of a reaction in the graphite furnace at the indicated low ambient pressures was emergence of bubbles from the liquid sessile drop and drifting of the drops during contact angle measurements until precipitates formed. Since Na was the redox reaction product, its presence as a vapor in order to nucleate and form bubbles indicated that its internal pressure was above the furnace ambient pressure of  $2.6 \times 10^{-4}$  Pa, but the bubble pressure was less than  $10^5$  Pa since bubbling did not occur with an ambient atmosphere of  $10^5$  Pa of He, also resulting in a limited weight loss. The boiling point of Na at  $10^5$  Pa is  $883^\circ\text{C}$  and at  $2.6 \times 10^{-4}$  Pa,  $121^\circ\text{C}$ . It is expected that the formation of these bubbles at the interface contributed to the mechanism for drifting of the drop. Drifting also occurred in the alumina furnace but not as extensively, and several bubbles appeared during a two-hour period. Drifting generally caused irregularly shaped drop peripheries.

A third sessile drop series of  $\text{NS}_2$ -LBL glass on Marz A iron was made at  $1000^\circ\text{C}$  for 2 hrs at ambient pressures of  $2.6 \times 10^{-4}$ ,  $6.6 \times 10^{-3}$ , 0.10 (all with a cold-trapped diffusion pump), 0.66 (just with mechanical pump), and  $1 \times 10^5$  Pa (in helium) in both furnaces (Table 3). The amount of reaction in the graphite furnace decreased with increase of the ambient pressure which is discussed later. In the alumina furnace, however, the amount of reaction increased with ambient pressure up to  $\sim 0.66$  Pa and then dropped significantly at  $1 \times 10^5$  Pa He; here, it is postulated that the  $P_{\text{O}_2}$  increased with ambient pressure except for He which had originally only 2-3 ppm of oxygen and was additionally gettered.

A cross-section of a sessile drop on Marz iron after 120 min at  $1000^\circ\text{C}$  in the graphite furnace is shown in Fig. 5a, and after 240 min in the

alumina furnace, in Fig. 5b; the lath-shaped crystals are cristobalite and the feathery globules in the zone next to the iron (Fig. 5a) and away from the interface (Fig. 5b) are mixtures of cristobalite and fayalite (identified by EDAX in SEM). The difference in microstructure and positions relative to the interface, and approximately the same % weight loss in both specimens, indicated the dominance of different reactions in the two furnaces.

#### B. Experiments With Other Iron Specimens

A number of experiments showed the sensitivity of the reactions to the nature or condition of the iron specimens. A comparison of the behavior of as-received Marz A iron, which was used in all of the previous experiments and used up, was made with other specimens: Marz I (as-received Marz A stored for 8 months in a vacuum desiccator at room temperature and  $\sim 1\text{Pa } P_{\text{O}_2}$ ), Marz II (Marz I annealed in graphite furnace at  $1050^\circ\text{C}$  and  $2.6 \times 10^{-4}\text{ Pa}$  ambient for 2 hrs), Marz III (Marz I annealed at  $1100^\circ\text{C}$  for 18 hrs), Marz B (second lot of as-received), Marz C (third lot of as-received), and Armco iron. These substrates were all tested with the same previously used  $\text{NS}_2\text{-LBL}$  glass at  $1000^\circ\text{C}$  and  $2.6 \times 10^{-4}\text{ Pa}$  for 2 hrs in both furnaces. The differences are significant as seen in Table 3.

Considering the conditions of the experiment the only factor that can vary is the  $a(\text{FeO})_{\text{int}}$  which is dependent on ambient conditions and strongly affects the extent of the redox reactions, as discussed later. The indications are that iron of high purity and unsaturated with oxygen can absorb oxygen from the ambient atmosphere during storage or aging. It would be expected that impure iron, with an excess of iron oxide, e.g. Armco, would not change and remain inert with time since  $a(\text{FeO})_{\text{int}}$  remains at one.

#### IV. REACTIONS

An analysis and interpretation of the results of this study suggest a number of oxidation and reduction (redox) reactions.

##### A. Oxidation of Iron by Atmospheric Oxygen

At 1000°C iron saturated with oxygen, and thus  $Fe_xO$  (hereafter referred to as FeO), on exposure to a partial pressure of oxygen above  $1.5 \times 10^{-10}$  Pa, which is the dissociation pressure of bulk FeO, results in oxidation of iron according to Eq.(1)



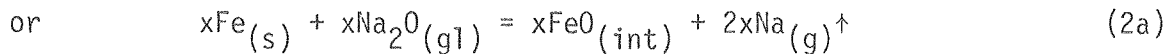
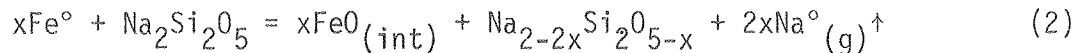
by diffusion through the forming oxide layer. Thus, this reaction is thermodynamically favorable in the alumina furnace and unfavorable in the graphite furnace.

Iron saturated with FeO has an activity of FeO of one ( $a(FeO) = 1$ ) and when it is free of FeO,  $a(FeO) = 0$ . If oxide unsaturated iron is placed in the alumina furnace, oxygen adsorbs on the surface and diffuses into the bulk iron with a corresponding increase of  $a(FeO)$  in the bulk with no growth of the oxide layer. On saturation, i.e. when  $a(FeO)$  becomes one, the oxide layer grows. With increase of  $a(FeO)$  the surface energy of the iron decreases to that of FeO.

If iron saturated with oxygen is placed in the graphite furnace, any FeO on the surface dissociates in the reverse direction of Eq.(1). After depletion of any oxide film, oxygen diffuses from the bulk toward the surface of the iron with a decrease of the  $a(FeO)$ . There is a corresponding increase of the surface energy of the iron to that of pure iron.

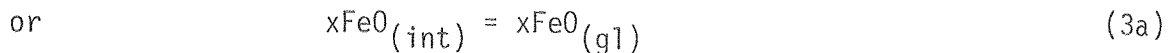
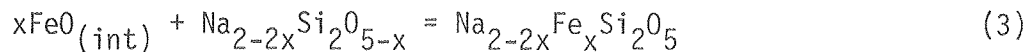
B. Oxidation of Iron by Reduction of Sodium in Glass

As indicated, redox reactions can occur at a glass-metal interface if thermodynamic equilibrium is not present. Hagan and Ravitz<sup>(5)</sup> working in  $\sim 2 \times 10^{-3}$  Pa vacuum in the range of 935 to 1000°C showed that iron reacts with sodium disilicate to form FeO and Na vapor. This reaction was confirmed in previous wetting studies in a graphite furnace<sup>(2,3)</sup> and in this study. The early stages of this reaction before precipitates form, in accordance with previous discussions, can be represented by Eqs. (2, 3 and 4).

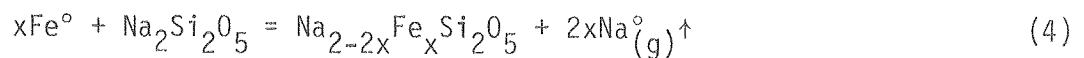


$$\Delta G = \Delta G_{1000}^\circ + RT \ln \frac{a(\text{FeO})_{\text{int}}^x (P_{\text{Na}})^{2x}}{a(\text{Na}_2\text{O})_{\text{gl}}^x} \quad (2b)$$

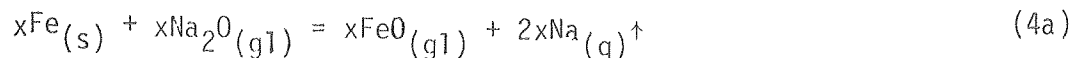
then



The net reaction is



or simplified as



The standard free energy at 1000°C ( $\Delta G_{1000}^{\circ}$ ) for reaction (2) was calculated to be 69.5 kcal/mol using data from JANAF Tables of Thermochemical Data<sup>(6)</sup>. Since  $\Delta G^{\circ}$  is positive, the reaction can only occur when the activity quotient or equilibrium constant in Eq.(2b) for the step reaction represented by Eq.(2) or (2a) is sufficiently smaller than one so that  $\Delta G_{1000}$  becomes negative.  $\Delta G^{\circ}$  for mixing for the step reaction (3) or (3a) is negative, as experimentally verified<sup>(7)</sup>. Thus, reaction (2) is the controlling step and the overall reaction (4) or (4a) can occur when  $a(\text{FeO})_{\text{int}}$  or  $a(\text{FeO})_{\text{metal}}$  and  $P_{\text{Na}}$  are small and  $a(\text{Na}_2\text{O})_{\text{gl}}$  is large. Actually, some of the FeO at the interface will diffuse into the iron if the  $a(\text{FeO})$  in the metal is  $< 1$  because of the thermodynamic driving force for equilibration of the  $a(\text{FeO})$  in the two phases at the interface. Essentially all of the FeO, however, will dissolve in the glass as indicated by Eq.(3) since the solubility of FeO in the glass is much greater than in the iron,  $\sim 44$  vs.  $\sim 0.01$  wt.%.

By assuming an activity of one for FeO and  $\text{Na}_2\text{O}$  only for thermodynamic calculations and a zero  $\Delta G$  for Eq. (2a), i.e. equilibrium under standard conditions,  $P_{\text{Na}}$  is calculated to be  $1.3 \times 10^{-4}$  Pa. Although this pressure exceeds the ambient pressure of the furnace permitting the formation of bubbles, considering the uncertainties of the data and the fact that the  $a(\text{Na}_2\text{O})_{\text{gl}}$  is less than one, the ratio of  $a(\text{FeO})_{\text{int}}/a(\text{Na}_2\text{O})_{\text{gl}}$  should be less than one and as small as possible for the reaction to proceed. Consequently, this reaction is more favorable in the graphite furnace because of its lower  $P_{\text{O}_2}$  on the basis of the discussion in Section IV-A.

From a thermodynamic viewpoint this reaction sequence will carry on as long as  $\Delta G$  of Eq. (2b) remains negative for the experimental conditions

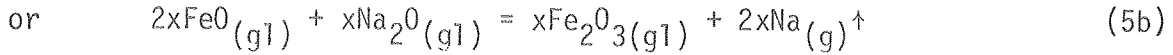
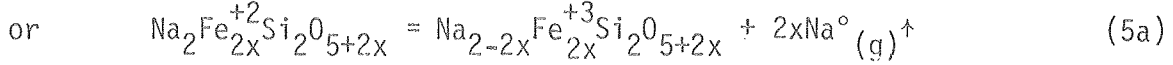
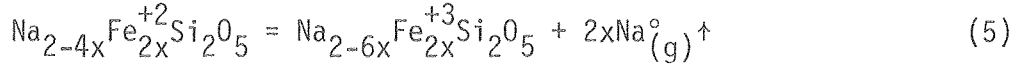
of temperature, time, total ambient pressure,  $P_{Na}$ ,  $P_{O_2}$ , and glass and metal structure and composition. The rate of the reaction will also be controlled by the conditions of the experiment. It would be expected that the minimum temperature for these reactions to occur readily is  $892^\circ\text{C}$ , the boiling point of Na.

### C. Oxidation of Ferrous Ions by Reduction of Sodium in Glass

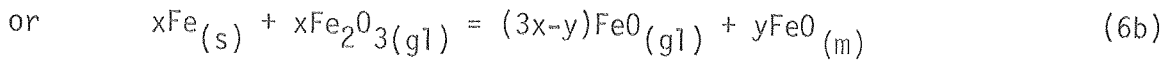
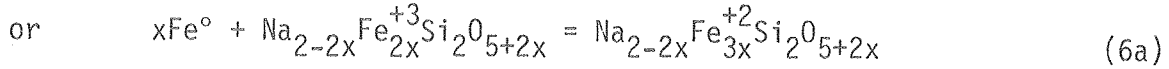
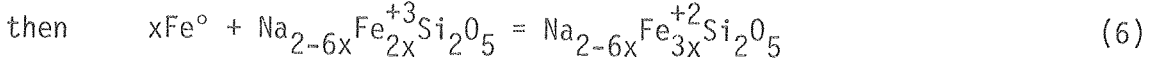
The loss in weight and a change in color from bluish to greenish-blue of a sessile drop of  $\text{NS}_2 + 10\% \text{FeO}$  on a fused  $\text{SiO}_2$  substrate in vacuum at  $1000^\circ\text{C}$  with no changes in a drop of  $\text{NS}_2$  with  $10\% \text{Fe}_2\text{O}_3$  under similar conditions (Table 2) indicate that another type of redox reaction occurred which involved the oxidation of  $\text{Fe}^{+2}$  in the glass to  $\text{Fe}^{+3}$  by reduction of  $\text{Na}^+$  to  $\text{Na}^0$ . Ferrous glasses are blue in color while ferric glasses are yellow-brown;  $\text{Fe}^{+2}$  in combination with  $\text{Fe}^{+3}$ , both being in six-fold coordination, give rise to a greenish color<sup>(9)</sup>. Some atmospheric oxidation undoubtedly occurred in the alumina furnace as deduced from a lesser weight loss than in the graphite furnace.

Some ferrous oxide initially enters  $\text{NS}_2$  glass by a redox reaction (2) if the  $a(\text{FeO})$  is less than one in the iron at the start, or by solution by the glass of an oxide film if  $a(\text{FeO})_{\text{int}} = 1$ . The subsequent redox reaction in the first case can be represented by Eqs. (5, 6 and 7), i.e. if  $\text{Fe}^{+2}$  enters the glass by redox reaction (2), and in the second case by Eqs. (5a, 6a and 7a), i.e. if  $\text{Fe}^{2+}$  enters as  $\text{FeO}$ . In general, this redox reaction in both cases is represented by Eqs. (5b, 6b and 7b).

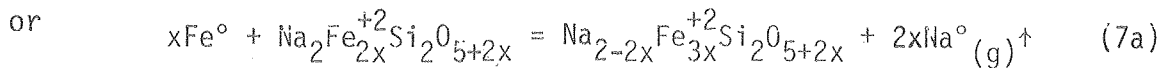
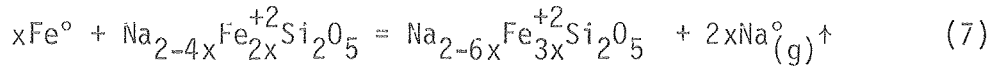




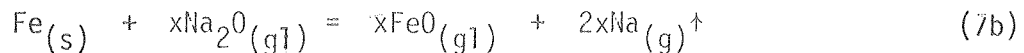
$$\Delta G = \Delta G_{1000}^\circ + RT \ln \frac{a(\text{Fe}_2\text{O}_3)_{\text{gl}}^x (p_{\text{Na}})^{2x}}{a(\text{FeO})_{\text{gl}}^{2x} a(\text{Na}_2\text{O})_{\text{gl}}^x} \quad (5c)$$



When  $a(\text{FeO})$  at the interface in the metal is one,  $x$  in Eq. (6b) is zero. If any  $\text{FeO}_{(\text{int})}$  forms, i.e.  $a(\text{FeO}) < 1$  and  $y \neq 0$ , it is dissolved by the glass according to Eq.(3a). This indicates that the same amount of FeO is introduced into the glass at the interface by reaction (6b) regardless of the value of  $x$ . The net reaction is



or simplified as



The  $\Delta G^\circ_{1000}$  for reaction (5b) was calculated<sup>(6)</sup> to be 78.3 kcal/mol. This reaction thus can only occur when the activity quotient in Eq.(5c) is sufficiently smaller than one so that  $\Delta G$  becomes negative. Calculating, as before, the  $P_{Na}$  is 0.018Pa which is favorable for this redox reaction to occur in either furnace. Thus reactions (4 and 7) can take place in the graphite furnace. The latter, however, is the only one that probably can take place in the alumina furnace when the metal is saturated with oxide ( $a(FeO)_{int} = 1$ ). The  $a(Fe_2O_3)_{gl}/a(FeO)_{gl}^2$  ratio must remain small and less than one because of a relatively low  $a(Na_2O)_{gl}$ . Since  $\Delta G^\circ_{1000}$  for reaction (6b) is -12.1 kcal when the  $a(FeO)$  in the metal is one,  $Fe_2O_3(gl)$  reacts readily with the iron to form  $FeO(gl)$  which keeps the ferrous/ferric ratio in the glass small and the reaction (5b) favorable and continuous; this reaction becomes even more favorable when the  $a(FeO)_{int}$  is less than one because of a favorable activity quotient for reaction (2). It is interesting to note that the net reaction (7b) is essentially the same as the net reaction (4b) although the step reactions are quite different which results in the different microstructures seen in Fig. 5.

In the case of redox reaction (2)  $FeO$  formed at the interface and was dissolved by the glass causing a diffusion gradient of  $Fe^{+2}$  from the interface into the liquid glass with a counter diffusion gradient of  $Na^+$  to the interface. Therefore, the continuing reaction sequence of a glass with dissolved  $FeO$ , with precipitates of cristobalite, and then with precipitates of cristobalite and fayalite was initiated at the interfaces as seen in Fig. 5a. In the case of redox reaction (5) or (5a) the first step of formation of  $Fe^{+3}$  takes place in the glass (with the reduced  $Na$  atoms diffusing out of the liquid) and the second step of formation of

$\text{Fe}^{2+}$  by reaction (6) or (6a) takes place at the interface. These reactions are expected to develop complex diffusion gradients of  $\text{Fe}^{+3}$  toward the interface and into the glass with probably a high point at some critical distance from the interface with a counter gradient of  $\text{Fe}^{+2}$  from the interface into the glass and a gradient of  $\text{Na}^+$  determined by charge balance requirements. The formation of  $\text{Fe}^{+3}$  in the glass took place at the distance from the interface at which the ratio of  $a(\text{Fe}_2\text{O}_3)/a(\text{FeO})^2$  was favorable for reaction (5) or (5a). The above reaction sequence was thus initiated at some distance from the interface as seen in Fig. 5b.

Generally, the same sequence of phase transformations occurs for Eqs. (5, 6 and 7) on continuation of the reactions as for Eqs. (2, 3 and 4) assuming that all of the ferric oxide formed by Eq.(5) or (5a) takes part in Eq.(6) as described in conjunction with the phase diagram of Fig. 4. If the amount of initial FeO dissolved is greater than ~15 wt%, a continuation of the reactions represented by Eqs. (5a, 6a and 7a) leads to the liquid being first saturated with fayallite and then also with cristobalite as indicated by the phase diagram. The change in composition at which saturation with any phase occurs due to the presence of  $\text{Fe}_2\text{O}_3$  in the liquid is not known since the only equilibrium phase diagram available is for the three components of  $\text{FeO-Na}_2\text{O-SiO}_2$ .<sup>(8)</sup>

## V. DISCUSSION

In a sessile drop experiment in which the two phases are in stable or metastable chemical equilibrium, the familiar Young-Dupre equation Eq.(9) indicates the equilibrium contact angle ( $\theta$ ) for the existing interfacial tensions which will remain constant with time.

$$\gamma_{SV} - \gamma_{SL} = \gamma_{LV} \cos \theta \quad (9)$$

$(\gamma_{SV} - \gamma_{SL})$  constitutes the driving force for wetting. In case of a reaction at the interface with the substrate as the active participant, i.e. undergoes a change in composition, such as reactions (2 and 6b with  $y > 0$ ), the increment of the specific free energy of the reaction at a given time ( $\Delta g$ ) around the periphery of the drop becomes a part of the driving force for wetting and  $\theta$  is thus reduced.  $\theta$  will also have some change with time since the reaction causes changes in compositions which in turn affect surface energies or tensions. If the reaction rate is fast or large enough, the  $\Delta g$  contribution is large enough so that the driving force for wetting exceeds  $\gamma_{LV}$  resulting in spreading<sup>(12)</sup>. For a reaction in which the substrate is the passive participant, i.e. undergoes no change in composition, such as reactions (5 to 7) the free energy of the reaction does not contribute to the driving force for wetting.

In the case of as-received Marz A iron Fig. 3 shows the change in  $\theta$  and the amount of the total Na lost with time at 1000°C in both furnaces indicating that the amount of reaction in a given time was greater in the graphite furnace (lower  $P_{O_2}$ ). On plotting the data as weight loss vs. contact angle in Fig. 6 the points fell essentially on a monotonic curve indicating that the change in composition of the glass was the critical factor in determining the change in driving force for wetting. The data also shows that there was a ( $\Delta g$ ) contribution to wetting due to reactions (2 and 6b with  $y > 0$ ) which remains essentially constant for a given composition of liquid glass. Reaction (6b) is dependent on reaction (6a). The rate of reactions (2) and (6b) is dependent on

the magnitude of  $a(\text{FeO})_{\text{int}}$  which is smaller (but not one) in the alumina furnace. Reaction (6a) is inherently slower than reaction (2) in vacuum because the Na produced in the former reaction is removed from the reaction site by diffusion and in the latter as a vapor by bubbling. The relative rates of these two reactions then determine the overall rate which, on the basis of the above, i.e. slower than reaction (2), is slower in the alumina furnace, but the driving force for wetting is essentially unaffected as long as  $a(\text{FeO})_{\text{int}} < 1$ . The relative rates also determine the microstructures observed in Fig. 5 and described earlier.

In the case of Armco iron, which has precipitates of  $\text{Fe}_x\text{O}$  and an  $a(\text{FeO})$  of one, the metal does not react with the glass according to reaction (2) but does react according to reaction (6) in which the metal is a passive participant.  $\text{Fe}^{+2}$  produced by reaction (6) can now participate in reaction (5) producing  $\text{Fe}^{+3}$  which can then react according to reaction (6). This cycle can repeat itself with a continuing increase of iron oxide in the glass. Since reaction (6) does not contribute its ( $\Delta g$ ) to the driving force for wetting because the metal is a passive participant, the contact angle does not change significantly and remains large as seen in Fig. 6.

The data indicate that Marz A iron on exposure to an ambient atmosphere with a  $P_{\text{O}_2}$  above the dissociation pressure of FeO absorbs oxygen even at room temperature (Marz I) causing an increase of  $a(\text{FeO})$ . Thus, variations in behavior of different shipment lots of Marz iron (B and C in Table 3) could be interpreted to be due to storage under different conditions and time before shipment. Heat treatment at a  $P_{\text{O}_2}$  below the dissociation pressure causes a decrease in oxygen content and  $a(\text{FeO})$ , as shown by Marz III.

Qualitative information on adherence was obtained by determining the ease with which the glass drops could be removed from the metal. Good adherence was always realized when the glass at the interface approached saturation with FeO due to redox reactions with the substrate. Reaction studies were continued until crystalline precipitates occurred for purposes of understanding and following the reactions. In practice, reactions would not be carried as far.

## VI. CONCLUSIONS

All redox reactions involving iron lead to the introduction of ferrous oxide into the glass at the interface. The semiquantitative kinetic studies, indicated that the reactions are sensitive to temperature, time and ambient pressure and  $P_{O_2}$ . The redox reactions are complicated since several can be going on simultaneously. The materials must be characterized as to activities of the various oxides and impurities. Experimental conditions must be kept constant to obtain correlatable kinetic data for a given series. The  $a(FeO)$  in the iron has been shown to be particularly critical. In order to completely understand the reactions and to obtain quantitative kinetic data, concentration profiles will be necessary of the elements concerned with submicron details at the interface.

Sessile drop experiments provide qualitative information in regard to the presence of certain reactions. Spreading or decrease of contact angles with time is an indication of a continuing reaction in which the substrate plays an active, i.e. undergoes a change in composition, instead of a passive role. Contact angle measurements thus become informative, particularly on a comparative basis such as in this study.

#### ACKNOWLEDGEMENTS

The authors are grateful to Professor Dr. Francisco Jose Valle (Institute of Ceramic and Glass, Arganda del Rey, Madrid, Spain) for performing the chemical analyses of the glasses.

This work was supported by the Director, Office of Energy Research, Office of Basic Energy Sciences, Materials Science Division of the U.S. Department of Energy under Contract No. W-7405-ENG-48.

REFERENCES

1. J.A. Pask and R.M. Fulrath, "Fundamentals of Glass-to-Metal Bonding: VIII," J. Am. Ceram. Soc., 45 [12] 592-96 (1962).
2. C.E. Hoge, J.J. Brennan and J.A. Pask, "Interfacial Reactions and Wetting Behavior of Glass-Iron Systems," J. Am. Ceram. Soc., 56 [2] 51-54 (1973).
3. J.J. Brennan and J.A. Pask, "Effect of Composition on Glass-Metal Interface Reactions and Adherence," J. Am. Ceram. Soc., 56 [2] 58-62 (1973).
4. J.J. Brennan and J.A. Pask, "Effects of Nature of Surfaces on Wetting of Sapphire by Liquid Aluminum," J. Am. Ceram. Soc., 51 [10] 569-73 (1968).
5. L.G. Hagan and S.F. Ravitz, "Fundamentals of Glass-to-Metal Bonding: VI," J. Am. Ceram. Soc., 44 [9] 428-29 (1961).
6. JANAF Thermochemical Data, The Dow Chemical Company, Thermal Research Laboratory, Midland, Mich., Sept. 30, 1967.
7. A.M. Lacy and J.A. Pask, "Electrochemical Studies in Glass: II, The System  $Fe_{0.95}O - Na_2Si_2O_5$ ," J. Am. Ceram. Soc., 53 [12] 676-79 (1970).
8. P.T. Carter and M. Ibrahim, "Ternary System  $Na_2O - FeO - SiO_2$ ," J. Soc. Glass Technol., 36 [170] 142-63T (1952).
9. W.A. Weyl, Coloured Glasses. Society of Glass Technology, Sheffield, England, 1951.
10. M.P. Borom and J.A. Pask, "Kinetics of the Interfacial Reaction and Diffusion Process in the System Iron-Sodium Disilicate Glass," Phys. Chem. Glasses, 8 [5] 194-202 (1967).



11. L. Shartsis and S. Spinner, "Surface Tension of Molten Alkali Silicates,"  
J. Research Natl. Bur. Standards 46, 385-90 (1951).
12. I.A. Aksay, C.E. Hoge and J.A. Pask, "Wetting Under Chemical Equilibrium  
and Nonequilibrium Conditions," J. Phys. Chem., 78 [12] 1178-83 (1974).

TABLE 1. CHEMICAL ANALYSIS OF GLASSES\*

Oxide Constituent	$\text{Na}_2\text{O}\cdot 2\text{SiO}_2$ ( $\text{NS}_2$ -LBL)	$\text{NS}_2+10\%\text{FeO}$	$\text{NS}_2+10\%\text{Fe}_2\text{O}_3$
$\text{SiO}_2$	64.38	58.81	58.74
$\text{Na}_2\text{O}$	33.85	30.62	30.28
$\text{FeO}$	-	8.81	0.35
$\text{Fe}_2\text{O}_3$	0.041	0.90	9.89
$\text{Al}_2\text{O}_3$	0.63	0.26	0.32
$\text{TiO}_2$	0.001	0.01	0.02
$\text{CaO}$	0.13	0.17	0.06
$\text{MgO}$	0.02	0.01	0.01
$\text{K}_2\text{O}$	0.05	0.03	0.05
$\text{B}_2\text{O}_3$	0.18	0.16	0.12

\*in weight percent.

TABLE 2. CONTACT ANGLES AND Na WT LOSS AT 1000°C  
AND  $2.6 \times 10^{-4}$  Pa FOR 1 HR VS TYPES OF MATERIAL

Glass	Substrate	Graphite Furnace		Alumina Furnace	
		Total Na % Wt Loss	Contact Angle	Total Na % Wt Loss	Contact Angle
NS <sub>2</sub> -LBL	Pt	0	15	0	16
NS <sub>2</sub> -LBL	Marz Iron	29.5	18	11.8	20
NS <sub>2</sub> -LBL	Fused SiO <sub>2</sub>	0	n.d.	0	n.d.
NS <sub>2</sub> -LBL	Armco	12.5	53	4.8	60
NS <sub>2</sub> +10%FeO	Fused SiO <sub>2</sub>	16.7*	n.d.	10.8*	n.d.
NS <sub>2</sub> +10%FeO	Fused SiO <sub>2</sub>	17.2*	n.d.	12.5*	n.d.
NS <sub>2</sub> +10%FeO	Fused SiO <sub>2</sub>	18.2*	n.d.	11.6*	n.d.
NS <sub>2</sub> +10%FeO	Marz Iron	100.0	0	91.7	0
NS <sub>2</sub> +10%Fe <sub>2</sub> O <sub>3</sub>	Fused SiO <sub>2</sub>	0 <sup>+</sup>	n.d.	0 <sup>+</sup>	n.d.
NS <sub>2</sub> +10%Fe <sub>2</sub> O <sub>3</sub>	Fused SiO <sub>2</sub>	0 <sup>+</sup>	n.d.	0 <sup>+</sup>	n.d.
NS <sub>2</sub> +10%Fe <sub>2</sub> O <sub>3</sub>	Marz Iron	100.0	0	91.7	0

\*Light green color

<sup>+</sup>Transparent yellow color

TABLE 3. CONTACT ANGLES AND Na WT LOSS AT 1000°C FOR 2 HRS  
VS PRESSURES AND TYPE OF METAL SUBSTRATE

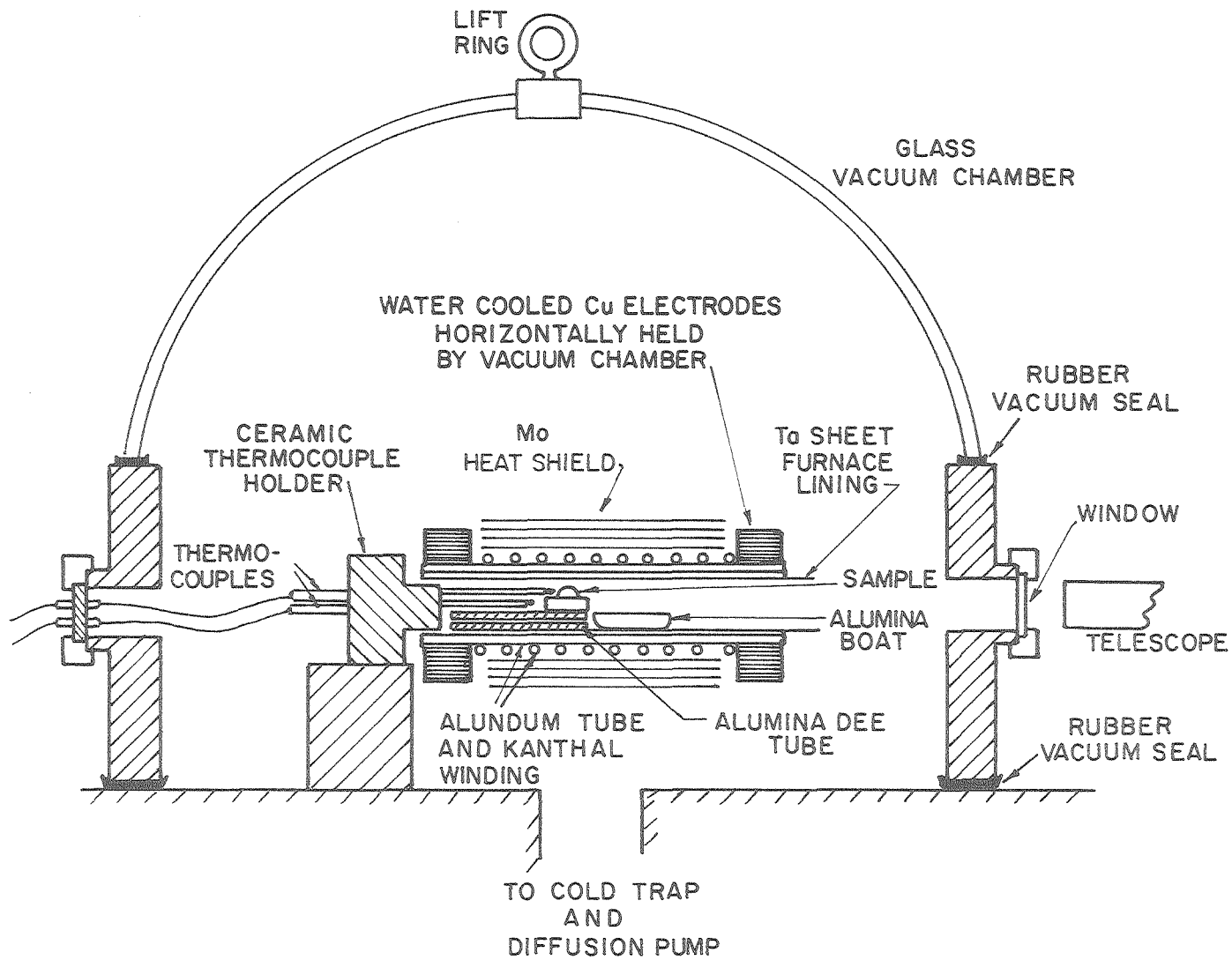
MATERIAL <sup>+</sup>	PRESSURE (Pa)	GRAPHITE FURNACE		ALUMINA FURNACE	
		Total Na % wt. loss	Contact angle	Total Na % wt. loss	Contact angle
Marz A*	1.01x10 <sup>5</sup> (He)	11.8	54	15.5	54
	0.66	24.6	52	77.8	5
	0.10	49.4	24	66.6	7
	6.6x10 <sup>-3</sup>	90.0	0		
	2.6x10 <sup>-4</sup>	95.4	0	57.4	10
Marz I	2.6x10 <sup>-4</sup>	15.7	55	8.1	55
Marz II	2.6x10 <sup>-4</sup>	18.8	48	23.2	21
Marz III	2.6x10 <sup>-4</sup>	96.0	0	56.6	15
Marz B*	2.6x10 <sup>-4</sup>	86.5	8	59.3	10
Marz C*	2.6x10 <sup>-4</sup>	35.6	44	9.6	56
ARMCO	2.6x10 <sup>-4</sup>	28.4	53	20.8	63

\*Three Marz iron specimens as-received: A-lot 26/52143 (used in experiments for Figs. 2 and 3), B-lot 26/57823, C-lot 26/2051

<sup>+</sup>NS<sub>2</sub>-LBL glass used in all experiments.

FIGURE CAPTIONS

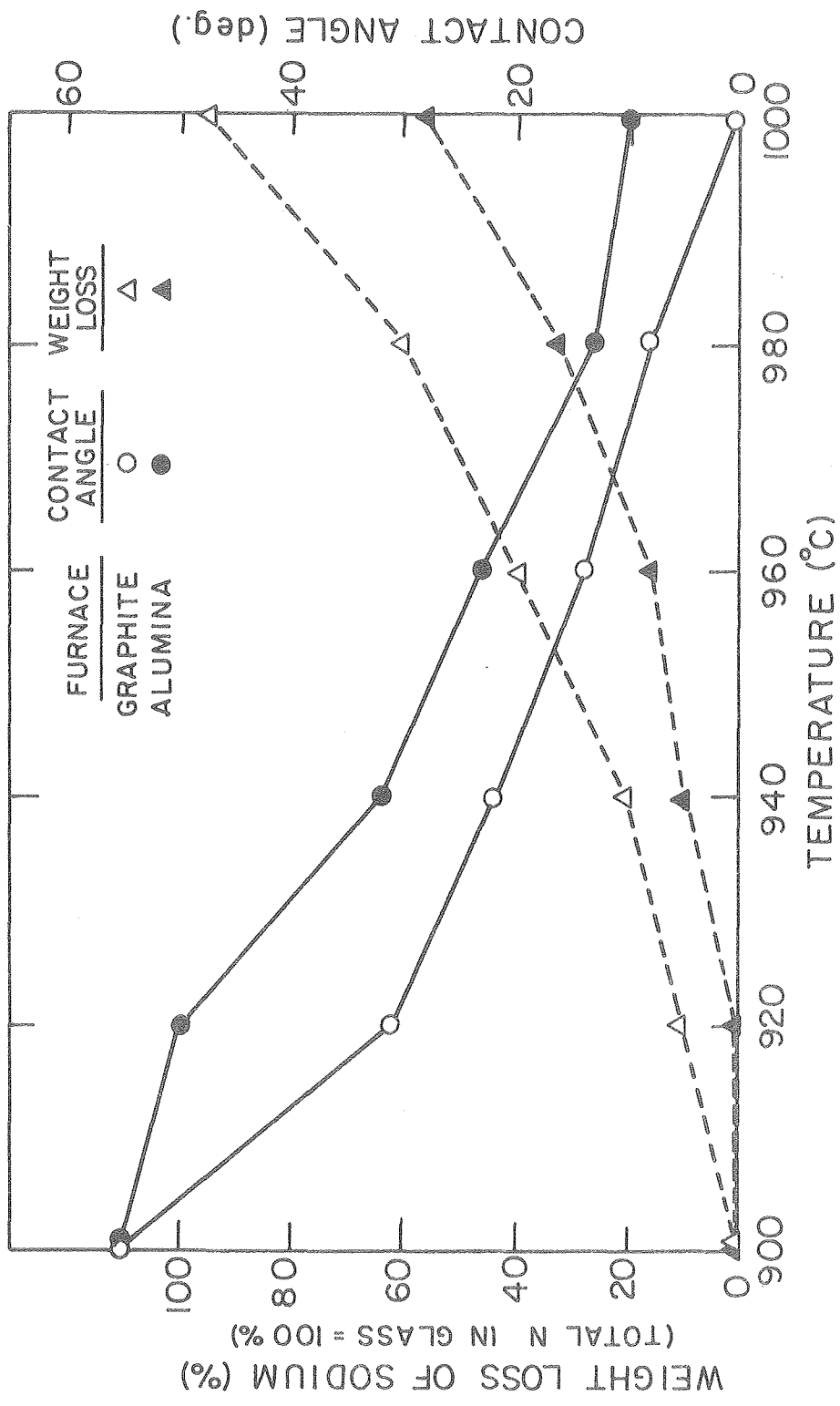
- Fig. 1. A schematic drawing of the alumina furnace (XBL 7811-6110).
- Fig. 2. Contact angles and % weight loss of total sodium from  $\text{NS}_2$ -LBL glass on Marz A iron at  $900^\circ\text{C}$  to  $1000^\circ\text{C}$  after 2 hrs at  $2.6 \times 10^{-4}\text{Pa}$ . (XBL 7910-7201)
- Fig. 3. Contact angles and % weight loss of total sodium from  $\text{NS}_2$ -LBL glass on Marz A iron vs. time from 10 to 250 minutes at  $1000^\circ\text{C}$  and  $2.6 \times 10^{-4}\text{Pa}$ . (XBL 7910-7200)
- Fig. 4. Isotherm for  $1000^\circ\text{C}$  on phase equilibrium diagram for  $\text{Na}_2\text{O}-\text{SiO}_2-\text{FeO}$  system. Composition line with squares represents  $\text{NS}_2$  glasses with progressive replacement of  $\text{Na}_2\text{O}$  by  $\text{FeO}$ . (XBL 722-6039)
- Fig. 5. Cross-sections of  $\text{NS}_2$ -LBL glass sessile drop on Marz A iron  
a) in graphite furnace, after 2 hrs at  $1000^\circ\text{C}$  with a total ambient pressure of  $2.6 \times 10^{-4}\text{Pa}$  and  $P_{\text{O}_2}$  of  $\approx 10^{-17}\text{Pa}$ , and b) in alumina furnace with  $P_{\text{O}_2}$  of  $\approx 10^{-7}\text{Pa}$  after 4 hrs at  $1000^\circ\text{C}$  at same ambient pressure. Approximately same weight of Na lost in both experiments. Specimens etched for 10 sec in 10% HF. Iron substrate at the bottom. See text for description of microstructures.
- Fig. 6. Contact angles vs. % weight loss of total sodium for  $\text{NS}_2$ -LBL glass on Marz A and Armco irons. The points marked as circles in squares are for Marz I.



-27-

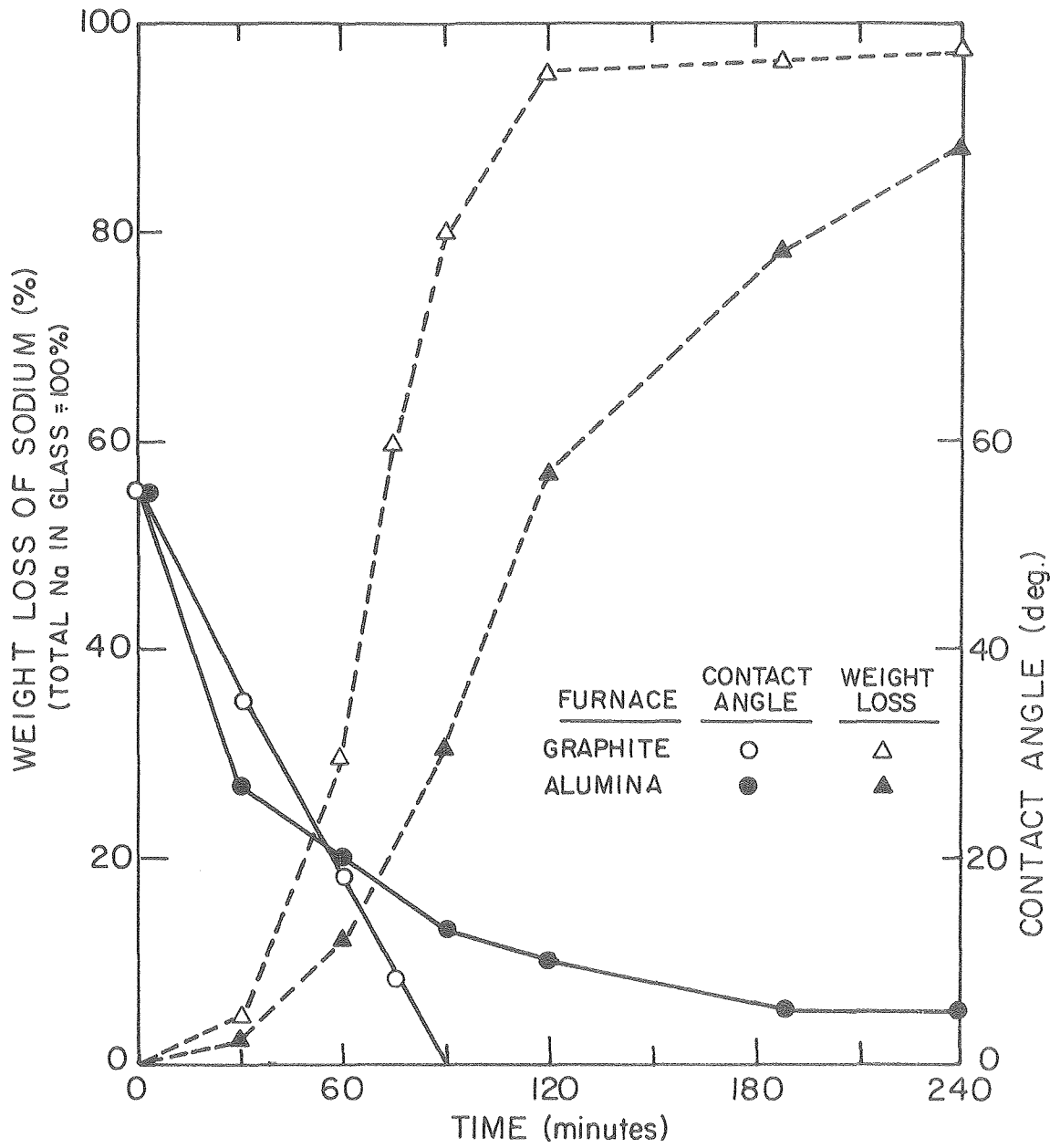
XBL7811-6110

Fig. 1



XBL7910-720I

Fig. 2



XBL 7910-7200

Fig. 3



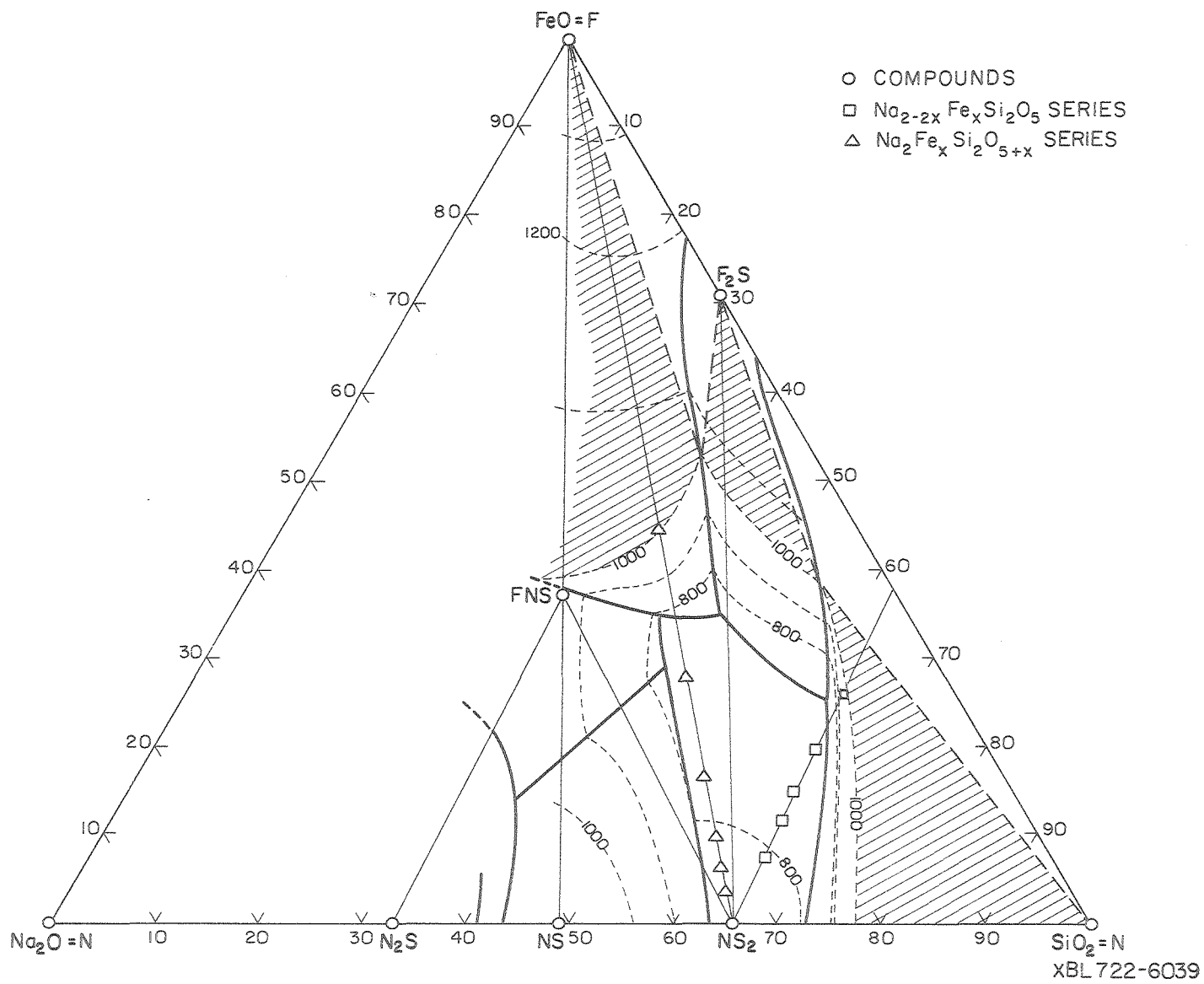
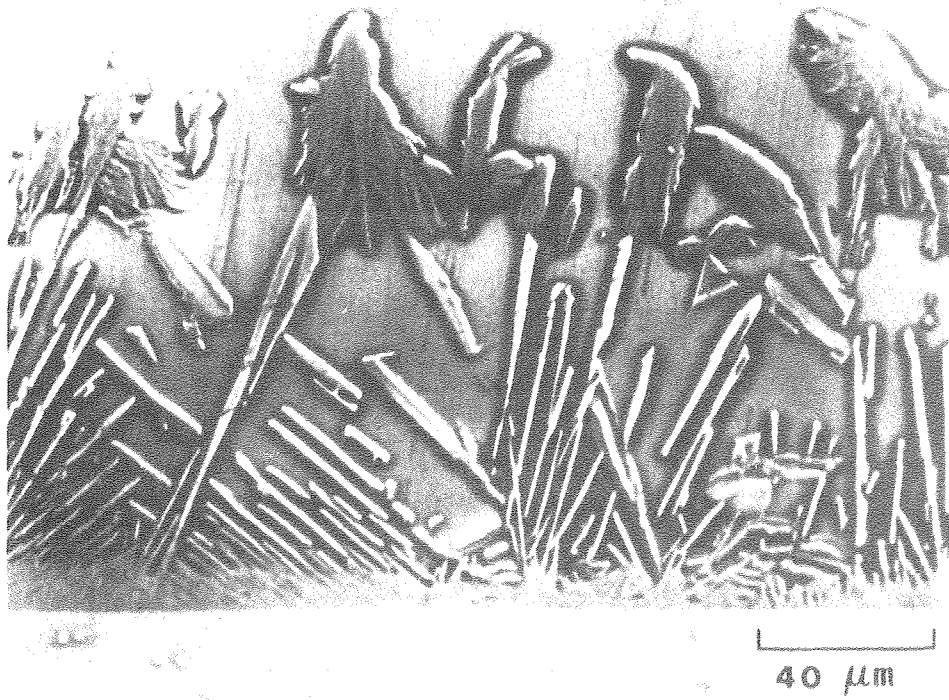
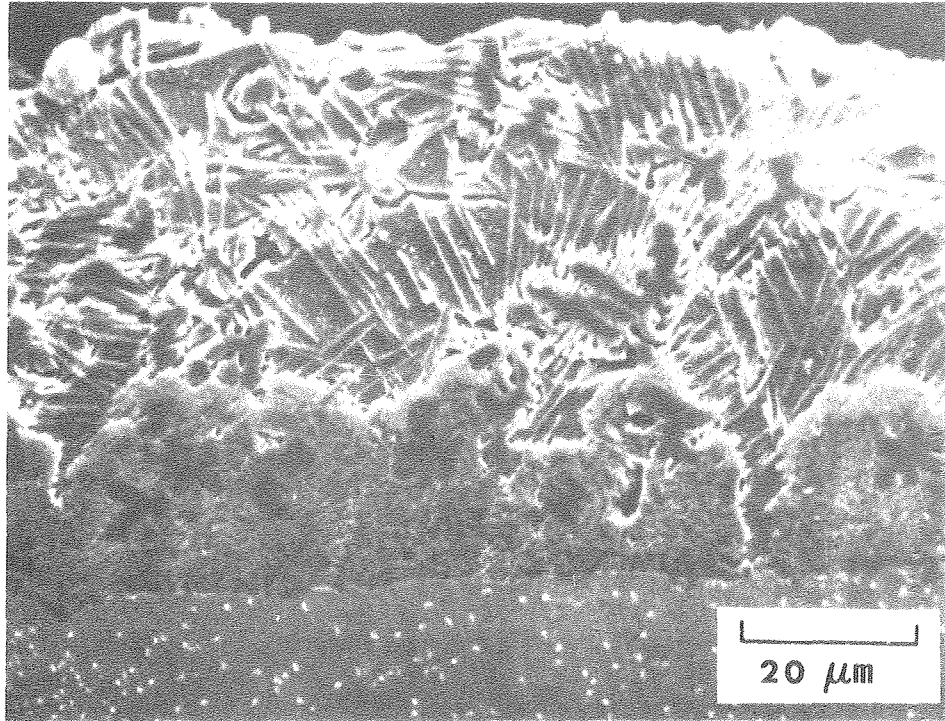


Fig. 4



XBB801 347

Fig. 5

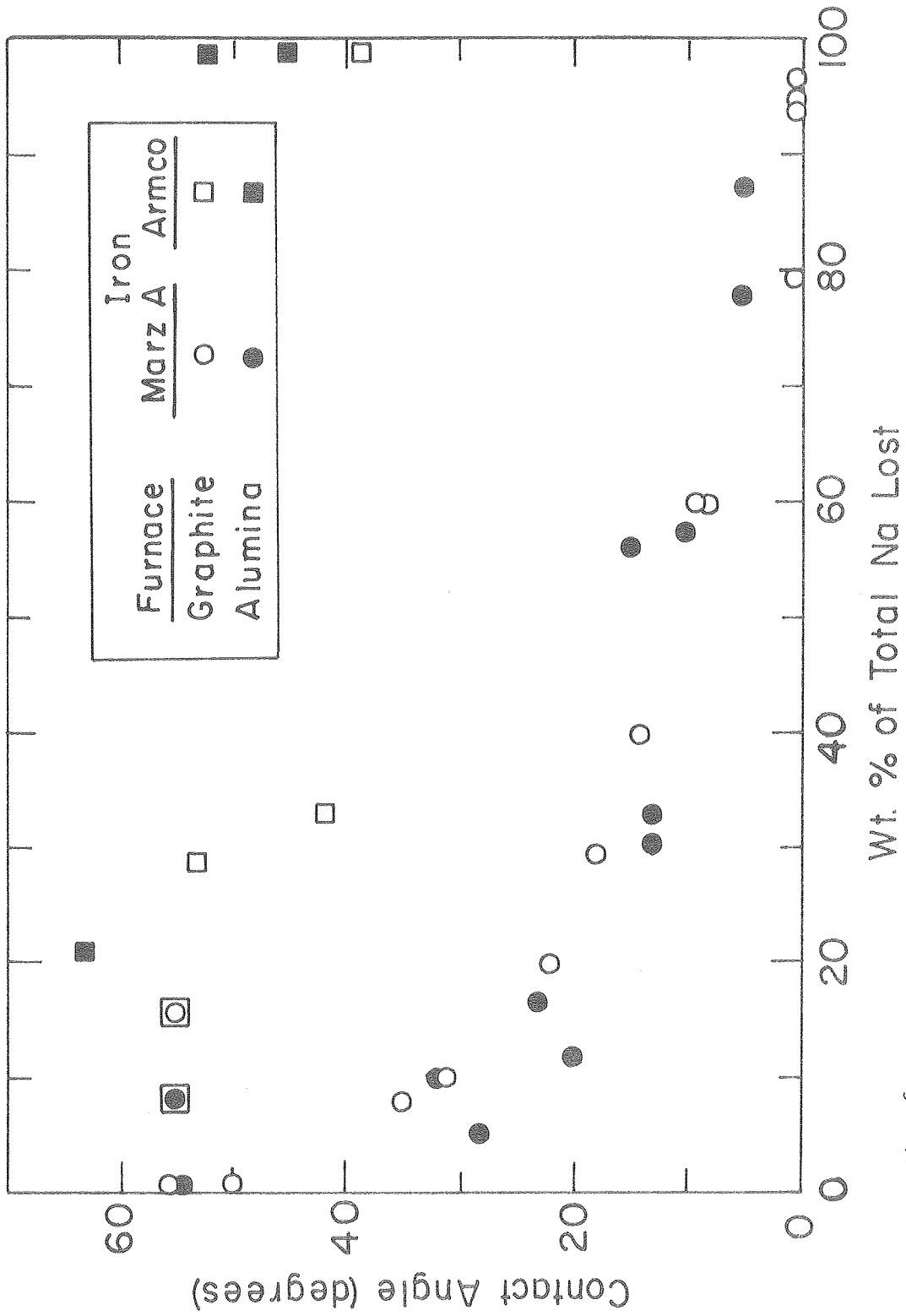


Fig. 6

XBL 80I-4550A